Molecular Parameters of siRNA–Cell Penetrating Peptide Nanocomplexes for Efficient Cellular Delivery

Alexander H. van Asbeck,[†,‡] Andrea Beyerle,[‡] Hesta McNeill,[‡] Petra H.M. Bovee-Geurts,[†] Staffan Lindberg,[§] Wouter P. R. Verdurmen,[†] Mattias Hällbrink,[§] Ulo Langel,[§] Olaf Heidenreich,[‡,*] and Roland Brock[†,*]

[†]Department of Biochemistry, Nijmegen Centre for Molecular Life Sciences, Radboud University Nijmegen Medical Centre, Nijmegen, 6525 GA, The Netherlands, [‡]Northern Institute for Cancer Research, Newcastle University, Newcastle upon Tyne, NE2 4HH, United Kingdom, and [§]Department of Neurochemistry, Stockholm University, S-10691, Stockholm, Sweden

ABSTRACT Cell-penetrating peptides (CPPs) are versatile tools for the intracellular delivery of various biomolecules, including siRNA. Recently, CPPs were introduced that showed greatly enhanced delivery efficiency. However, the molecular basis of this increased activity is poorly understood. Here, we performed a detailed analysis of the molecular and physicochemical properties of seven different siRNA–CPP nanoparticles. In addition, we determined which complexes are internalized most efficiently into the leukemia cell-line SKNO-1, and subsequently inhibited the expression of a luciferase reporter gene. We demonstrated effective complexation of siRNA for all tested CPPs, and optimal encapsulation of the siRNA was achieved at very similar molar ratios independent of peptide charge. However, CPPs with an extreme high or low overall charge proved to be exceptions, suggesting an optimal range of charge for CPP–siRNA nanoparticle formation based on opposite charge. The most active CPP (PepFect6) displayed high serum resistance but also high sensitivity to decomplexation by polyanionic macromolecules, indicating the necessity for partial decomplexation for efficient uptake. Surprisingly, CPP–siRNA complexes acquired a negative ζ-potential in the presence of serum. These novel insights shed light on the observation that cell association is necessary but not sufficient for activity and motivate new research into the nature of the nanoparticle–cell interaction. Overall, our results provide a comprehensive molecular basis for the further development of peptide-based oligonucleotide transfection agents.

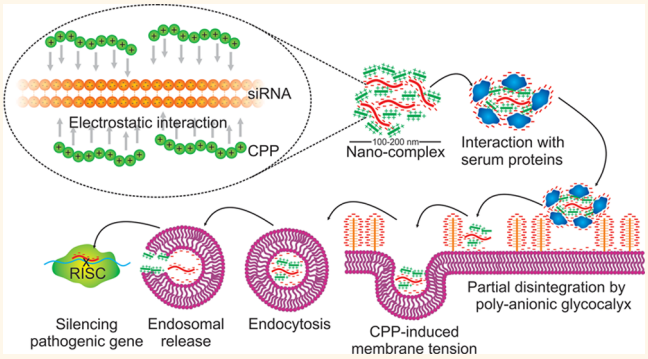

KEYWORDS: drug delivery · siRNA therapeutics · cell-penetrating peptides · transfection · electrostatic · oligonucleotide nanoparticles

Activity and specificity remain major challenges in the design of classical small molecule drugs, and at present, only a limited number of pathophysiologically relevant proteins can be targetted.[1] With the discovery of siRNA and miRNA, strategies to specifically target pathogenic proteins on the post-transcriptional level have emerged.[2] The highly specific nature of these oligonucleotides and the clear-cut design principle demonstrate their potential as drugs of the future. However, the problem of efficient cellular delivery has not yet been resolved.

Due to the hydrolytic sensitivity and poor cellular uptake of 'naked' polyanionic oligonucleotides,[3] most delivery strategies currently under investigation are based on formulations that protect the oligonucleotides from degradation by hydrolytic enzymes and at the same time mediate cellular delivery. However, strategies that conjugate siRNA to the delivery vehicle have lacked efficacy *in vivo* and have been shown to activate innate immunity.[4] Therefore, nanoparticle approaches are currently the main focus. These approaches comprise liposomes,[5] micelles,[6] polymeric nanoparticles,[7] nanospheres,[8] complex formation of oligonucleotides with antibody-protamine conjugates,[9] and cell-penetrating peptides (CPPs).[10–13]

At this point, it is still not clear which of these strategies will ultimately show clinical

* Address correspondence to R.Brock@ncmls.ru.nl, olaf.heidenreich@newcastle.ac.uk.

Received for review November 20, 2012 and accepted April 21, 2013.

Published online April 21, 2013
10.1021/nn305754c

success. Ease of synthesis, formation and stability of the formulation, toxicity and *in vivo* efficiency are the criteria against which each formulation strategy has to be evaluated. Furthermore, many formulations that show activity in tissue culture have been shown to lose activity in the presence of serum.[2]

CPPs are a very promising group of delivery vectors. These molecules consist of short cationic or amphipathic sequences of about 5–30 amino acids, which have the ability to induce effective cellular uptake and delivery of a conjugated or electrostatically bound cargo.[14] Prominent members are the arginine-rich 11 amino acid Tat peptide[15] derived from the HIV transactivator protein, and the oligoarginines.[16,17] The lactoferrin-derived CPP hLF is a 22 amino acid peptide which shares functional characteristics with oligoarginines, yet requires cyclization *via* a disulfide bridge for activity and achieves efficient uptake at a lower arginine density.[18] Transportan and the shorter TP10 were the first members of a family of amphipathic CPPs developed with a particular focus on oligonucleotide delivery.[19] Recently, it was shown that stearylated TP10 analogs show superior activity in oligonucleotide transfection,[20] which the next-generation PepFect6 further enhanced through the coupling of trifluoromethylquinoline moieties to the peptide.[21] Alternatively, with PepFect14 the lysines and isoleucines of TP10 were replaced by ornithines and leucines, respectively, which also improved the transfection efficiency.[22] In addition to having different physicochemical characteristics, these peptides show differences in the molecular mechanisms of cell association, uptake and intracellular trafficking, although the molecular and functional details of these differences are poorly defined.[23]

CPP-mediated delivery of small molecules, peptides and proteins generally involves a covalent attachment of the cargo to the peptide, which is problematic for siRNA delivery. Spontaneous electrostatic complexation of the polyanionic siRNA and the cationic/amphipathic CPP renders chemical coupling reactions inefficient.[24,25] Furthermore, the incorporation of the guide strand of the siRNA into the deep-pocket of the RNA-induced silencing complex, which is essential for the silencing mechanism, is disrupted by covalently attached molecules.[2] For these reasons, CPP-mediated siRNA delivery is usually achieved by means of electrostatic interaction between anionic siRNA and cationic CPP. A molar excess of CPP over siRNA is used to neutralize the negative charge and to protect the siRNA from serum enzymes. The characteristics of siRNA–CPP complexes are largely dependent on the exact ratio of CPP to siRNA used in the formulation, the Molar Ratio (MR).

Four key parameters are thought to affect the transfection efficiency of CPP–siRNA complexes: size, charge, stability and cell association. These parameters affect endosomal uptake of the CPP–siRNA complexes, the main route of internalization for macromolecular complexes.[26,27] However, endosomal uptake alone is insufficient to predict functional siRNA delivery.[23]

Current literature shows a lack of understanding of how these characteristics differ between individual CPPs. Especially the relevant molecular characteristics that distinguish an effective siRNA–CPP complex from an inactive one remain to be defined.

This study aims to investigate the relationship between physicochemical parameters and biological activity for a range of paradigmatic representatives for arginine-rich and amphipathic CPPs. The physicochemical parameters include particle size, surface charge and complex stability; the biological activity consist of cell association and uptake, toxicity and target gene silencing. Human leukemic SKNO-1 cells expressing the *RUNX1/ETO* fusion gene were employed as the target cell line.[28] The formation of fusion oncogenes cannot, at the time of writing, be adequately addressed with small molecule drugs, and therefore, siRNA directed against these fusion oncogenes are considered a potential therapeutic modality. For this reason, these cells presented a highly relevant, application-oriented test case.[29]

We will show that siRNA transfection efficiency is a function of complexation, cell association and induction of cellular uptake, and decomposition of the CPP–siRNA complex in the presence of polyanions. For some functionally relevant parameters, clear-cut linear relationships with individual molecular characteristics were identified. Overall, these results provide a comprehensive molecular basis for the further development of peptide-based oligonucleotide transfection agents.

RESULTS AND DISCUSSION

The Size of CPP–siRNA Complexes Is Dependent on the Molar Ratio and Medium Composition. The size of nanoparticles is an important characteristic, since it has been shown to substantially affect their pharmacokinetics and pharmacodynamics.[30,31] Ideally, CPP–siRNA complexes should be smaller than 200 nm to ensure optimal endocytic uptake and diffusion through tissue *in vivo* by the permeation retention effect (EPR).[32] We therefore addressed the impact of the molar ratio of peptide over oligonucleotide and the buffer conditions on the size of the resulting CPP–siRNA complexes. In addition to TP10 and its analogs PepFect 6 (PF6) and PepFect 14 (PF14), R9, the Tat peptide, the hLF peptide and an R9-hLF hybrid peptide were included. For the latter, the high cationic charge was thought to drive complexation by strong electrostatic interaction with siRNA. TP10 and the PepFects are amphipathic CPPs for which all positive charge is carried by lysine residues and by trifluoroquinolines as in the case

of PepFect 6 (Table 1). The rest of the peptides belonged to the class of arginine-rich CPPs. The number of positive charges, which are considered vital for the complexation of oligonucleotides and initiation of cellular uptake, ranged from 4 for TP10 to 16 for R9-hLF (Table 2).

CPPs are much smaller ($MW_{CPP} = 1.4 \times 10^3$ to 4.4×10^3 g/mol) and have a lower absolute charge (N 4−16) than the siRNA ($MW_{siRNA} = 1.3 \times 10^4$ to 1.5×10^4 g/mol, with a negative charge P of about 40); therefore, the CPPs were used in molar excess over siRNA for complex formation. For each peptide, the size of the resultant CPP−siRNA complexes at several molar ratios were measured in water and 5% glucose, reflecting the conditions used for the clinical application of drugs (Figure 1A,B). The individual peptides showed very different behaviors. In the case of R9, R9-hLF and PF14, the size was relatively independent of the molar ratio and ranged between 150 and 200 nm. However, Tat, TP10, PF6 and hLF showed a correlation between size and molar ratio (Figure 1A). Interestingly, all four peptides showed a size maximum at an N/P (N = positively charged amino acids, P = phosphate groups on siRNA) ratio from 2 to 5 (Figure 1B). The size of the polyplexes involving PF14 is consistent with data obtained by transmission electron microscopy of PF14 oligonucleotide complexes in contact with cells.[33,34]

All the peptides tested showed little variation in complex size beyond an N/P ratio of 5, with the exception of TP10, which formed the largest complexes with a maximum size of 2 μm. Remarkably, there was no correlation between the characteristics of complex formation and the overall characteristic of the CPP (arginine-rich/amphipathic) as illustrated by the different behaviors of TP10, PF6, and PF14.

The addition of 5% glucose to water had a negligible effect on complex size (data not shown). In contrast, in a physiological salt solution (150 mM) or a standard tissue culture medium, complex size increased considerably (150 mM NaCl, ratio to salt-free conditions ~1.4−4, RPMI1640, ratio to salt-free conditions ~1−3.5) in comparison to the salt-free conditions (Figure 1C and Supporting Information Figure 2). The size increase in the presence of physiological concentrations of salt (150 mM NaCl or serum-free cell culture medium) was more pronounced at higher molar ratios. This result suggests that the salt ions form bridges between CPP molecules, resulting in looser and bigger particles. The addition of serum to the tissue culture medium yielded smaller complexes that were comparable in size to the ones obtained in salt-free conditions (20% FCS, ratio to salt-free conditions ~0.6−1.3).

Optimal Molar Ratio of CPP to siRNA. Complexation of siRNA by CPP is intended to protect the siRNA against nuclease-mediated degradation.[35] For this reason, the encapsulation of siRNA by the individual CPP was investigated by a gel retardation assay. Naked siRNA is small enough to pass through the pores of a 3% agarose gel, while siRNA complexed with CPP will cause retention or a severe retardation of shift (Figure 2A and Supporting Information Figure 3). Quantification of the degree of siRNA encapsulation revealed a typical saturation pattern. Notably, for hLF, R9, Tat, PF6 and PF14, complete (>98%) encapsulation of siRNA was generally achieved near molar ratio 50, seemingly irrespective of the charge or mass of the peptide (Figure 2B,C). Only TP10 (>98% at Molar Ratio 99.3) and R9-hLF

TABLE 1. Amino Acid Sequences of the Used Cell-Penetrating Peptides

name	sequence[a]
hLF	Acetyl-**K**CFQWQ**R**NMR**KVR**GPPVSC**KR**-NH_2
R9	Acetyl-**RRRRRRRRR**-NH_2
R9-hLF	Acetyl-**RRRRRRRRRK**CFQWQ**R**NMR**KVR**GPPVSC**KR**-NH_2
Tat	Acetyl-G**RKKRR**Q**RRR**PQ-NH_2
TP10	Acetyl-AGYLLG**K**INL**K**ALAALA**KK**IL-NH_2
PF6	Stearyl-AGYLLGK(K(K_2(**tfq$_4$**)))INL**K**ALAALA**KK**IL-NH_2
PF14	Stearyl-AGYLLG**K**LL**OO**LAAAAL**OO**LL-NH_2

[a] Sequences are given in one-letter code, O indicates ornithine. Peptides were N-terminally acetylated or stearylated and C-terminally amidated (−NH_2). Positively charged lysine, ornithine and arginine residues are shown in bold-face. Disulfide bond-forming cysteine residues in hLF and R9-hLF are underlined. PF6 carries four trifluoroquinoline moieties (tfq), coupled *via* a lysine dendrimer.

TABLE 2. Summary of Properties for 7 Different CPP for siRNA Delivery

									by 200 nM siGL3	
CPP	mass[a]	N	charge at pH 7.4[b]	IC_{50} of heparin replacement assay	% siRNA release after 20 h serum 37 °C	ζ-pot. aqueous (mV)	ζ-pot. serum (mV)	MOLAR RATIO at 98% siRNA encap.	% luciferase knockdown	% membrane tox. rel. to 2% triton X-100
hLF	2719	7	+5.71	0.91	57%	7.8	−4.6	50.1	19%	5%
R9-hLF	4122	16	+14.7	1.31	41%	21.0	−8.0	58.0	19%	12%
R9	1424	9	+8.73	1.53	51%	14.8	−5.5	48.0	15%	6%
Tat	1621	8	+7.76	1.10	54%	25.7	−5.8	47.7	13%	2%
TP10	2184	4	+2.82	0.63	45%	12.4	−10.8	99.3	26%	19%
PF6	4412	11	+10.0	0.85	32%	25.5	−11.2	51.1	85%	9%
PF14	2407	5	+4.79	0.54	32%	46.7	−11.0	49.6	45%	17%

[a] Calculated. [b] Estimated by modeling of the peptide sequences in MarvinSketch software 2011, ChemAxon.

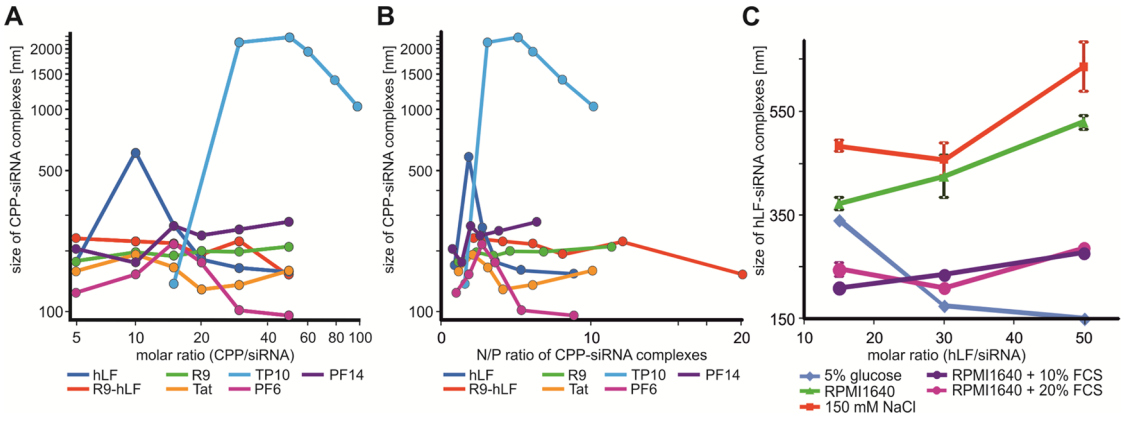

Figure 1. The relationship between the size of CPP–siRNA complexes and the (A) molar ratio, (B) N/P ratio and (C) medium composition. The size of CPP–siRNA complexes, formed by mixing of CPP and siRNA (MR 5, 10, 15, 20, 30, 50 for all, except TP10 = MR 15, 30, 50, 60, 80, 100) in water supplemented with 5% glucose (A and B) or in salt-containing medium (C; MR 15, 30, 50), was measured by DLS (n = 3, Supporting Information Figure 1 is a more detailed representation of this data and includes standard deviations). (B) The N/P ratio displays the charge-corrected ratio between CPP (N = positively charged amino acids) and siRNA (P = phosphate groups). (C) Results obtained for the hLF peptide in different solutions are shown. Results obtained for the other CPPs were qualitatively similar (Supporting Information Figure 2).

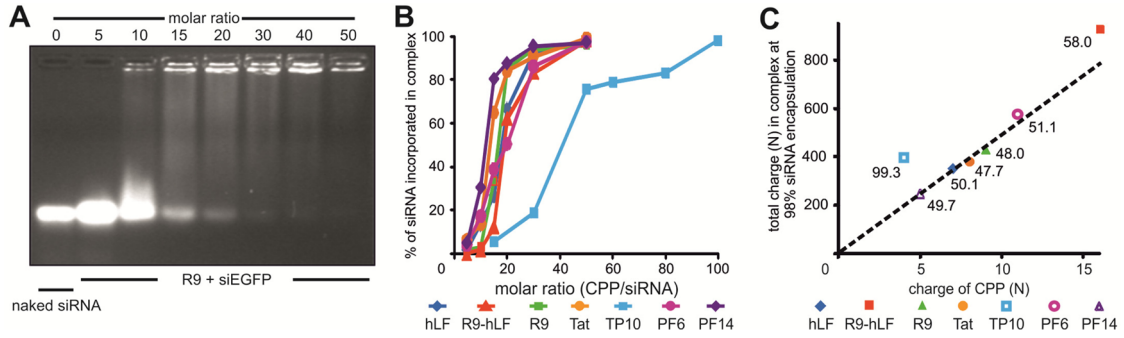

Figure 2. Correlation of siRNA encapsulation with molar ratio and N/P ratio. (A) Gel shift assay for siRNA encapsulation as exemplified for R9. siRNA was visualized by GelRed staining (n = 1). (B) siRNA encapsulation plotted against molar ratio as derived from gel shift assays shown in panel A. (C) Correlation of the charge of the CPP and the total charge of the complex when 98% siRNA encapsulation was achieved. The corresponding molar ratios at which this encapsulation was achieved are depicted next to the respective marker; the line represents an approximation of molar ratio 50.

(>98% at Molar Ratio 58.0) proved to be exceptions. In the case of the highly cationic R9-hLF, more siRNA may be required to overcome repulsion of the cationic CPP, whereas the low positive charge of TP10 is likely to result in a low binding capacity for siRNA. We propose a model in which electrostatic forces generated by the opposite charge of CPP and siRNA are balanced by the reciprocal electrostatic repulsion of CPP molecules and also by steric constraints. Considering concerns on the biological safety of highly cationic polymers, these results demonstrate that in a certain configuration extra positive charge does not add a functional benefit.[36]

Negative ζ-Potential of CPP–siRNA Complexes in the Presence of Salts and Serum Proteins. With respect to charge, the excess of CPP over siRNA generally used in CPP–siRNA complexes results in an overall positive ζ-potential when measured in aqueous buffers. This surface charge is commonly believed to allow interaction with the polyanionic glycosaminoglycans on the cell-surface.[37] However, it was recently observed that, in serum-containing media, complexes formed with the CPP PepFect14 had a negative surface ζ-potential.[34] Uptake was mediated by scavenger receptors, a type of cell surface receptor involved in the cellular uptake of negatively charged macromolecules.[34] As a result of this observation, we addressed the effect of the environment on the ζ-potential of the complexes (Figure 3). In a 5% glucose solution, all peptides showed a steady increase in ζ-potential with increasing molar ratio over a range of 15, 30, and 50. At high molar ratios (equal to the molar ratio at 98% siRNA encapsulation), a pronounced positive ζ-potential was found for all peptides. We observed large differences between the different CPPs that did not correlate with the charge of the corresponding peptide. In addition, TP10 and the hLF displayed negative ζ-potentials at molar ratios 30 and 15, respectively, but positive ζ-potential at higher molar ratios.

In contrast, the ζ-potentials of all of the CPP–siRNA complexes were negative in the presence of serum (Figure 3). DLS measurements demonstrated that the CPP–siRNA complexes were much bigger in salt and

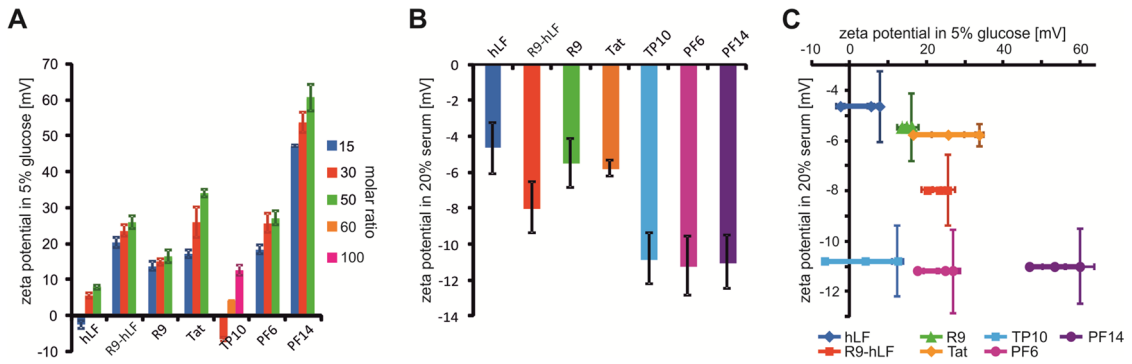

Figure 3. ζ-Potential of CPP−siRNA complexes in 5% glucose (A) and serum-supplemented medium (B). The ζ-potential of CPP−siRNA complexes formed in 5% glucose or in RPMI1640 + 20% serum was measured by dynamic light scattering. The correlation between both ζ-potentials is displayed in panel C. For all peptides, molar ratio 15, 30, and 50 in 5% glucose are displayed (TP10; MR 30, 60 and 100), but for serum conditions, only the highest molar ratio (all CPPs = MR 50, except TP10 = MR 100), which is indicated by the vertical error bars (n = 3) was measured.

only slightly bigger in serum-containing solution suggesting an interaction of the CPP−siRNA complex with salts and proteins in the solution, which affected the structure and size of the complex.

Based on the ζ-potential in serum-containing media, the CPPs could be subdivided into 3 distinct classes. The arginine-rich CPP R9, Tat and also hLF had a relatively weak negative ζ-potential. The R9-hLF peptide, which is much larger and contains the largest number of positive charges per peptide, showed a stronger negative ζ-potential. The amphipathic TP10-derived peptides (TP10, PF6 and PF14) formed the third class of peptides, with the strongest negative ζ-potentials in the presence of serum, relatively similar to one another. These results demonstrate that the acquisition of a negative ζ-potential is a general characteristic of CPP−siRNA complexes and not restricted to TP10-derived CPP. The reduction in particle size in the presence of serum in comparison to salt alone strongly suggests that charged serum proteins alter the structure of the complex. Furthermore, the change in ζ-potential indicates that serum proteins interact with the outer layer of the complex. Demonstration of the negative ζ-potential has great consequences for our understanding of the behavior of CPP−siRNA complexes in the bloodstream and their interaction with cells. Our results demonstrate that the potential involvement of scavenger receptors for uptake as was shown for PF14 by Ezzat *et al.* should be addressed for other CPPs as well.[34]

The Stability of CPP−siRNA Complexes in the Presence of Serum and Polyanions. During circulation in the bloodstream or infiltration of tissues, CPP−siRNA complexes will not only interact with serum proteins, but also encounter polyanions such as heparan sulfates present on cell surfaces. Interaction with these polyanions might result in disintegration of the complexes, resulting in siRNA release. In the bloodstream, premature disintegration would be detrimental, leading to degradation of the siRNA. In fact, lack of serum resistance is one of the most serious shortcomings of current siRNA delivery strategies.[2] However, ultimately, siRNA has to be released from the CPP−siRNA complexes, and polyanions in the glycocalix and/or inside the cell could play an important role in this disintegration. The role of polyanions in siRNA release *in vivo* is not yet known and it is therefore of interest to investigate the stability of the CPP complexes toward polyanions in correlation with their efficacy.

The stability toward heparin mimicking heparan sulfate proteoglycans as the major polyanions on the cell surface was measured in a heparin replacement assay. Generally, there was a strong positive correlation between the charge of the CPP (N) and the resistance to heparin-induced decomplexation (Figure 4). Interestingly, two separate lines could be drawn (R^2 = 0.98 and R^2 = 0.89), with PF14 at the intersection. R9, Tat and hLF fell into one group, R9-hLF and PF6 into the second group. R9-hLF complexes showed a lower electrostatic stability than expected based on the N of this peptide. This finding may be due to charge repulsion within the peptide and/or the ability to engage more readily in interactions with heparin. As stated above, R9-hLF also required a higher molar ratio for full siRNA encapsulation. In contrast, TP10 stability was higher than expected for the given number of positive charges. This CPP has a dispersed cationic charge. Therefore, the high stability of the complex in the presence of polyanions is surprising. The amphipathic nature of the peptide might be the cause of the high stability.

Serum stability of the CPP−siRNA complexes was then assessed over a 20 h time course (Figures 5A). The cationic CPPs Tat, R9 and hLF showed a pronounced siRNA release already after 1 h indicating a rapid disintegration of the CPP−siRNA complex.

Complexes formed with the much larger and more cationic R9-hLF peptide were more resistant to the effects of serum. The amphipathic peptide TP10 showed an intermediate resistance to serum. Very interestingly, PF6 and PF14 also showed a strongly improved

resistance to serum up to 20 h incubation at 37 °C. We found a clear linear correlation ($R^2 = 0.90$) between the ζ-potential in serum conditions and the sensitivity to serum. Those complexes with the most negative potential were also the most resistant in the presence of serum at 37 °C.

The increased resistance of PF6 and PF14 to disintegration confirms earlier observations.[21] Both amphipathic CPPs contain stearyl residues, which support the formation of micellar structures and are likely to enhance serum stability. In all our experiments, complexes were formed at CPP concentrations above the critical micellar concentration (critical micelle concentration), which is about 0.5 μM for PF6.[38] The molecular basis for the linear correlation of negative ζ-potential of the particles in serum conditions and the resistance to serum-mediated decomplexation is not fully clear. PepFect14 oligonucleotide complexes were shown to assume a negative ζ-potential already in the presence of salt.[22] It is unclear whether this ζ-potential protects the CPP oligonucleotide complexes from the interaction with serum components or, alternatively, induces the formation of a protective layer of serum proteins that protects the CPP−siRNA complexes from degradation.

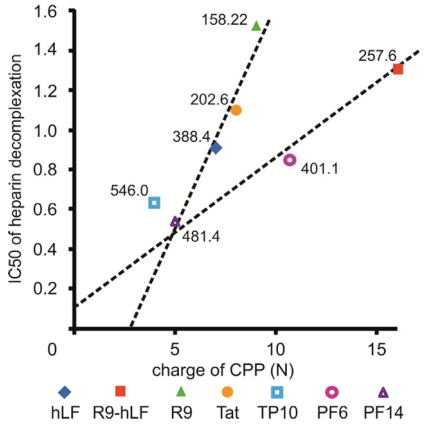

Figure 4. Correlation between the charge of the CPP (N) and the electrostatic stability of the complex. Electrostatic stability was tested by introducing a range of heparin (*i.e.*, polyanion) concentrations in CPP−siRNA complex containing solutions. The release of siRNA by the CPP was measured by incorporation of intercalating dye in released siRNA. Fluorescence was measured with a spectrophotometer ($n = 3$). Molecular weight of the CPP to N ratios are given next to the respective markers (MW/N = molecular weight per charged residue). $IC_{50} = 0.075 \times N$, $R^2 = 0.98$, $p = 0.077$ for R9-hLF, PF6 and PF14. $IC_{50} = 0.24 \times N - 0.90$, $R^2 = 0.86$, $p = 0.059$ for hLF, R9, Tat and PF14.

Heat inactivated serum did not induce any disintegration (data not shown) suggesting that degradation of the CPP may contribute to the disintegration of the CPP−siRNA complexes. A comparison of degradation kinetics of R9 and TP10 in 10% serum showed that R9 is degraded with a half-life of 1−2 h while TP10 is less susceptible to degradation (Supporting Information Figure 4). This result indicates that for the arginine-rich peptides degradation plays a role in the disintegration of complexes, while for the PepFects micelle formation and peptide stability may synergize in complex stability.

Cell Association and siRNA Activity. Having characterized the physicochemical properties of the CPP−siRNA complexes, we were interested in the relationship with biological activity. Fluorescently (Cy5.5) labeled siRNA was mixed with the various CPPs and incubated at 37 °C with cells of the leukemic SKNO-1 cell line in the presence of serum. Cell association was visualized by confocal microscopy (Figure 6) and quantified by flow cytometry (Figure 7 and Supporting Information Figure 5). Considerable differences in the distribution and extent of cell association were detected between different CPPs. hLF showed a strong association with the plasma membrane with highly focal accumulations. This association was stronger than for PF6 and PF14. R9-hLF and TP10 exhibited similar patterns

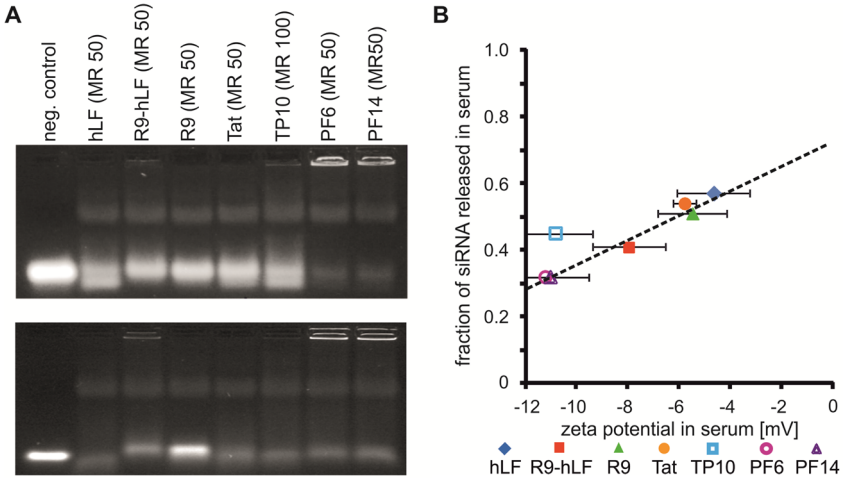

Figure 5. Serum stability of CPP−siRNA complexes. (A) Gel retardation assays for determination of siRNA release in 100% serum after 1 h (top panel) and 20 h (bottom panel) ($n = 1$) at 37 °C. (B) Correlation of siRNA release from CPP−siRNA complexes to the ζ-potential in serum ($n = 3$); fraction degraded = 0.71 + 0.036 × ζ-potential in serum, $R^2 = 0.90$, $p < 0.01$ (1 h).

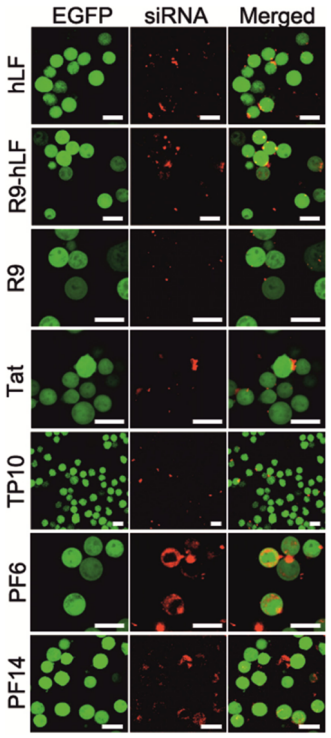

Figure 6. Cell association of CPP–siRNA complexes to SKNO-1 cells in serum conditions. Confocal images of cell-association of Cy5.5 (red) labeled CPP-complexed siRNA to GFP expressing SKNO-1 cells (green). Images were taken after 1 h incubation of 200 nM siRNA and corresponding CPP concentration (depends on molar ratio) with SKNO-1 cells at 37 °C. Scale bar = 20 μm (molar ratio of all CPP = 50, except TP10 = MR100). Note that not all cells express EGFP at high level; in a minority of cells, EGFP expression was lost.

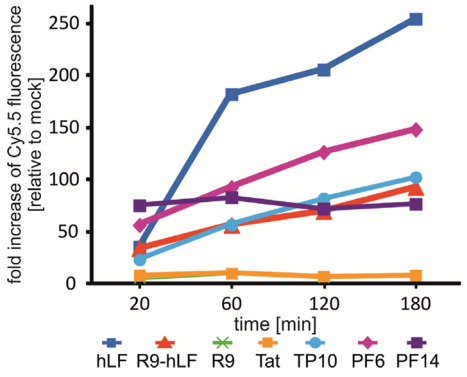

Figure 7. Quantification of cell-association of Cy5.5 labeled CPP–siRNA complexes to SKNO-1 cells by flow cytometry (geometric mean, *n* = 1). SKNO-1 cells were incubated between 20 min and 3 h with fully formed CPP–siRNA complexes (end concentration = 200 nM siRNA; molar ratio of hLF = 50, R9-hLF = 50, R9 = 50, Tat = 50, TP10 = 100, PF6 = 50, PF14 = 50).

of punctuate membrane association as hLF, but the extent of cell association was much smaller.

Neither the arginine-rich CPP Tat and R9 nor naked siRNA showed significant association with SKNO-1 cells. For hLF, R9-hLF and PF6, time-dependent increases in cell association were observed. For PF6 and PF14, an extensive cytosolic distribution of the labeled siRNA was seen, combined with some focal accumulations on both the cell membrane and in the cytoplasm. This distribution of fluorescence suggests an endocytosis-like uptake mechanism for PF6 and PF14, followed by a relatively early endosomal escape. Especially amphipathic and arginine-rich peptides differ significantly in the exact interaction with the plasma membrane and the type of endosomal uptake.[23] Surprisingly, cell association of CPP–siRNA complexes did not correlate with the ζ-potential of the corresponding complexes under serum conditions. For instance, TP10, PF6 and PF14 showed only small differences in the ζ-potentials in serum conditions but major differences in uptake. In addition, hLF-siRNA complexes had the least negative ζ-potential of all complexes analyzed and showed the strongest cell association. These results suggest that a specific conformation or the binding of specific serum proteins might be the key determinant for cell association.

The efficacy of siRNA delivery by the individual CPPs was addressed using a luciferase reporter assay. Functional release and activity of luciferase siRNA were determined in the presence of serum in SKNO-1 cells stably expressing luciferase. In these experiments, a siRNA targeting the leukemic fusion gene *RUNX1/ETO* served as negative control. Large differences in the efficacy of different CPP–siRNA complexes were found with only the amphipathic peptides showing substantial potency. PF6 was the most potent cellular delivery vehicle for siRNA with knockdown levels ranging from 60% at 50 nM siRNA to 85% at 200 nM, closely followed by PF14, with a 70% reduction in luciferase activity at 200 nM luciferase siRNA. The other CPP–siRNA formulations showed only minimal efficacy at concentrations up to 200 nM siRNA (Figure 8A).

In agreement with earlier studies, cell association was not a strong predictor for transfection activity.[39] hLF-siRNA complexes, in spite of having the highest cell-association over time, showed little siRNA-mediated down-regulation of luciferase expression. In contrast, the PepFect peptides PF6 and PF14 showed only limited cell association, but a much higher transfection efficacy which correlated with the cytoplasmic distribution of the peptides. The low *in vitro* activity of hLF should therefore be attributed to low endosomal uptake and escape.

Cytotoxicity. The metabolic cytotoxicity of CPP–siRNA complexes *in vitro* was tested by the WST-1 assay and membrane toxicity by LDH release assays (Figures 8B,C). Cells were incubated for 24 h for the WST-1 assay to assess long-term toxicity and the LDH release incubation was restricted to a 4 h period. At lower concentrations of up to 200 nM siRNA, minimal toxicity (<10%) was found for hLF, R9 and Tat-containing complexes, whereas both R9-hLF and TP10 showed

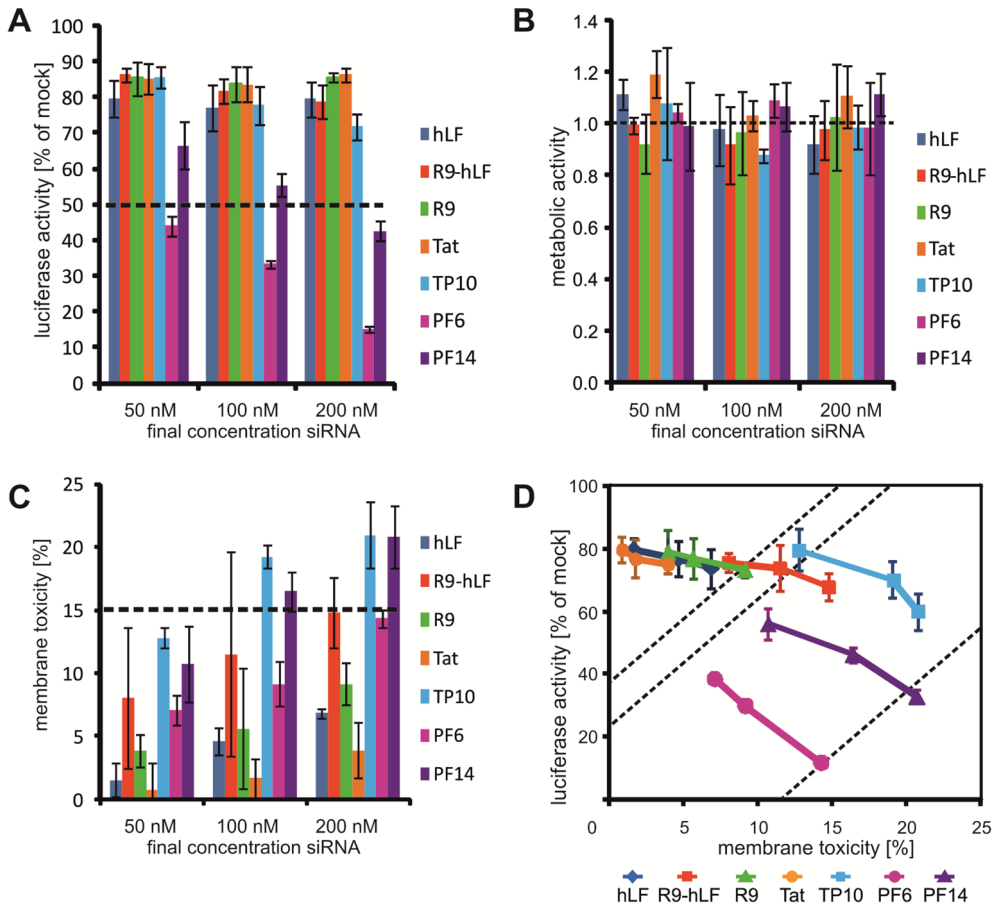

Figure 8. ***In vitro*** **silencing activity and** ***in vitro*** **membrane toxicity of CPP−siRNA complexes in SKNO-1 cells. For each peptide, three siGL3 concentrations (50, 100, and 200 nM) encapsulated by CPP (molar ratio of hLF = 50, R9-hLF = 50, R9 = 50, Tat = 50, TP10 = 100, PF6 = 50, PF14 = 50) were incubated with SKNO-1 cells. (A)** ***In vitro*** **activity was measured 48 h after incubation with CPP−siRNA particles by luciferase assays and normalized to control siRNA-treated cells (CPP-siAGF1 = Mock). (B) Overall cytotoxicity was determined by WST-1 assays. Cells were exposed to the nanoparticles for 4 h in a volume of 25 μL after which 75 μL of serum-containing medium was added and the incubation continued for another 20 h (Mock = only siRNA in 5% glucose). No significant differences compared to the Mock were found. ($p > 0.05$) (C) Membrane toxicity was tested by the LDH assay after 4 h incubation with nanoparticles at low serum concentrations (1%); results are displayed relative to 2% Triton X-100 treated cells. (D) Comparison of CPP activity** ***vs*** **membrane toxicity.**

up to 20% toxicity despite a lack of efficacy in siRNA delivery. The amphipathic peptides PF6 and PF14 showed at 200 nM toxicities of 15% and 20%, respectively, with PF14 being comparable to TP10. However, PF6 showed a smaller increase in toxicity for a given increase in efficacy (Figure 8D). At higher complex concentrations corresponding to 500 nM and 1 μM siRNA, all complexes showed significant membrane disturbance and cytotoxicity with up to 70% membrane toxicity (Supporting Information Figure 6), which correlated with substantial cell death, determined by trypan blue staining. The higher membrane toxicity of the amphipathic PepFect peptides (PF6 and PF14) in comparison to Tat is in line with earlier comparisons of Tat and TP10.[26] Interestingly, the membrane toxicity of these peptides was almost similar to the toxicity displayed by TP10, indicating that toxicity is caused by the amphipathic α-helical nature of the peptides and not by the stearyl tails on PF6 and PF14 or the pH titratable chloroquine moieties on PF6, which both present promising strategies for enhancing endosomal release of other CPP.

CONCLUSIONS

This study demonstrates that siRNA transfection efficiency of CPP oligoplexes is a function of complexation, resistance to serum proteins, decomposition in the presence of polyanions and induction of cellular uptake, which ultimately leads to release of functional oligonucleotides inside the cell. Comparison of TP10 with PF6 and PF14 indicates that stearylation plays a major role in several of these characteristics. It will therefore be interesting to explore to which extent stearylation will also benefit the characteristics of hLF, the CPP that showed the strongest membrane association of CPP−siRNA complexes. Our studies also revealed some clear-cut linear correlations of molecular characteristics that will form the basis for rational design strategies for more active CPP (Table 2). On one hand, a negative ζ-potential of complexes in the

presence of serum is correlated with a strong protective effect toward degradation by serum. On the other hand, a rather low charge of the CPP promotes decomplexation by polyanions. In addition, these insights into the interdependence of *in vitro* molecular characteristics and *in vivo* activity could constitute highly powerful *in vitro* predictors of *in vivo* activity. It will be interesting to explore to what degree these fundamental concepts, defined for CPPs here, do also hold for lipoplexes and polyplexes.

METHODS

Oligonucleotide and Peptide Synthesis. Lyophilized siGL3 (against *Photinus pyralis* luciferase, sense 5′-CUUACGCUGAGUACUUCGAdTdT-3′, antisense 5′-UCGAAGUACUCAGCGUAAGdTdT-3′), siAGF1 (against the acute myeloid leukemia fusion gene RUNX1/ETO,[28] sense 5′-CCUCGAAAUCGUACUGAGAAG-3′, antisense 5′-UCUCAGUACGAUUUCGAGGUU-3′) and siEGFP (5′-GGCUACGUCCAGGAGCGCACC-3′ and 5′-GGUGCGCUCCUGGACGUAGCC-3′) were obtained from Eurofins MWG Operon (Ebersberg, Germany) and aliquoted in 20 μL hybridization buffer (25 mM HEPES pH 7.5, 100 mM NaCl) at a final concentration of 100 μM before storage at −20 °C. Here, siAGF1 served as a negative control. Aliquots were thawed when needed and further diluted to a working concentration of 20 μM by adding 80 μL of hybridization buffer for analysis of complexation or 80 μL of RPMI1640 medium. The CPP nonaarginine (R9), human lactoferrin (hLF), the hybrid R9-hLF peptide, the Tat peptide and the TP10 peptide were purchased from EMC Microcollections (Tübingen, Germany). PepFect 6 (PF6) and PepFect 14 (PF14) were synthesized as described previously.[21,22]

Complex Formation. Formation of complexes was achieved by adding 7.5 μL of 20 μM siRNA to increasing volumes of 100 μM CPP solution and RNase-free water or RPMI1640 medium to obtain a final volume of 150 μL. This solution was thoroughly mixed (by repeated pipetting) and incubated for 30 min at room temperature. For serum conditions, fetal bovine serum (not heat-inactivated, Sigma) was added separately after complexation. Again, the total volume was kept at 150 μL. For dynamic light scattering (DLS) and gel retardation, the end concentrations of siRNA were kept constant (1 μM) while the total amount of CPP differed for the different molar ratios. For use in tissue culture experiments, amounts of reagents were scaled as required.

Determination of Particle Size and ζ-Potential. The size of freshly prepared siRNA−CPP complexes was measured by DLS. A total of 70 μL of the solution containing complexes was pipetted into a disposable 70 μL micro UV cuvette, and sizes were determined at room temperature at setting "medium" in a Nano ZS Zetasizer (Malvern Instruments, Malvern, U.K.). ζ-Potentials were measured in the same machine. To that end, freshly prepared samples (total volume 100 μL) were diluted 10-fold with RNase free 5% glucose solution to a total volume of 1 mL. A total of 750 μL of that solution was slowly injected into a folded capillary ζ-potential cuvette. For measurements in serum conditions, freshly prepared samples were diluted 1:10 with RPMI1640 + 20% FCS. Both size and ζ-potential mean values were determined from three independent measurements. As controls, blanks with only water, with 20% FCS and with siRNA and FCS were measured.

Gel Retardation Assay. An electrophoretic mobility shift assay (gel retardation assay) was used to assess the incorporation of the siRNA by the CPP into the complexes. For each solution, prepared at different molar ratios of siRNA and CPP, 20 μL was mixed with 4 μL of 6× DNA loading buffer (10 mM Tris-HCl (pH 7.6), 0.03% bromophenol blue, 0.03% xylene cyanol FF, 60% glycerol, 60 mM EDTA) separated on a 3% agarose gel containing GelRed Stain (Biotium, Cambridge, U.K.) in 0.5 M TBE buffer for 1 h at 70 V. The gel was photographed in a Bio-Rad transluminator (UV).

Polyanion (Heparin) Replacement Assay. To evaluate the stability of the CPP−siRNA complexes, a polyanion decomplexation assay, also called polyanion competition assay, was performed. Complexes were freshly prepared as described above in a total reaction volume of 650 μL. The complexes were equally distributed over 13 wells (50 μL/well) of a black, flat-bottom 96-well plate. To each well, 50 μL of 1× SyBr Gold solution (TE buffer, pH 7.8) was added and incubated for 10 min in the dark at room temperature. A serial dilution of heparin (MW 14 000) in RNase free water was prepared and 100 μL of each dilution was added followed by an incubation of 20 min in the dark at room temperature. Naked siRNA treated the same as the complexes and complexes without heparin were included as positive and negative controls, respectively. Samples were read in a fluorescence Omega FluoStar plate reader (BMG Labtech, Aylesbury, U.K.) with an excitation wavelength at 495 nm and an emission wavelength at 530 nm. Values are represented as percentage of fluorescence (RFU) of naked siRNA, after correction of the autofluorescence of the untreated complexes. For comparison and validation, heparin decomplexation was also analyzed by a gel retardation assay as described above.

Tissue Culture Conditions. Cells were grown at 37 °C, 5% CO_2, in a humidified atmosphere. Human leukemic SKNO-1 cells were cultured as described previously[29] and were lentivirally transduced to express a luciferase-IRES-EGFP construct under control of an SFFV promoter.

Determination of Cell Association and Uptake. To measure cell association, 200 μL of a suspension of 5 × 10^5 SKNO-1 cells/mL was incubated at 37 °C, 5% CO_2 and 95% humidity with 50 nM Cy5.5-labeled siRNA complexed with the optimum protecting molar ratio of each of the CPPs. A total of 50 μL of cell suspension was

removed at the indicated time points, diluted with 250 μL of PBS containing 1% FCS and analyzed in a FACS-Calibur (BD, Oxford, U.K.).

For confocal microscopy, 200 μL of cell suspension with 5×10^5 cells/mL was transferred into chambered coverslips and incubated (37 °C, 5% CO_2, 95% humidity) with 50 nM Cy5.5-labeled siRNA complexed with the particular CPP. After 1 h, the cells were imaged with a Zeiss LSM 700 Flexible Confocal Microscope, using a C-Apochromat 40×/1.2 W Corr UV−vis-IR for overviews and a C-Apochromat 63×/1.20 W Corr UV−vis-IR for the enlargements. GFP was excited with the 488 nm line of an argon ion laser and fluorescence was detected over 492−522 nm; Cy5.5 was excited with a 633 nm HeNe laser and emission was detected over 667−732 nm. Cells were maintained on a heated stage and imaged at low laser intensities to maintain viability and reduce photobleaching.

Determination of *in Vitro* Silencing Activity. To assess the knockdown efficiency of the CPP−siRNA complexes, luciferase activity of SKNO-1 cells treated with complexes was compared to the activity in cells treated with the same siRNA by electroporation as described previously.[29] After a 24, 48, 72, and 96 h incubation at 37 °C, 5% CO_2 and 95% humidity for 24 h, 1×10^5 cells were taken for the luciferase luminescence assay.

For the CPP−siRNA treatment of cells, 250 μL of a cell suspension of 4×10^6 cells/mL was added to the wells of a 12-well plate containing the complexes in glucose 5%. Cells were incubated for 4 h at 37 °C, 5% CO_2 and 95% humidity before addition of 2 mL of fresh medium. After 24, 48, 72, and 96 h, 1×10^5 cells were removed for the luciferase assay.

Luciferase Assay. The freshly taken cell suspension was centrifuged (1 min, 700*g*) and the remaining supernatant removed. Cells were centrifuged for 1 min at 700*g*, washed twice with 1 mL of sterile PBS and centrifugation at maximum speed for 1 min followed by addition of 50 μL of 1× lysis buffer (Promega, Southampton, U.K.) to the cell pellet. After incubation for 10 min at 37 °C, samples were frozen at −80 °C for at least 20 min. An aliquot of 10 μL of each sample, after correction for protein content by Bradford assay, was added into a 96-well Lumiplate (Perkin-Elmer, Cambridge, U.K.). Each sample was prepared and measured in triplicate. Seconds before reading the plate, 50 μL of luciferase assay reagent (Promega) was added to all wells in the same order as the reading direction. Samples were read with a luminescence reader (Perkin-Elmer) at 562 nm with 10 measurements per well.

Determination of Cytotoxicity. A serial dilution of cells ranging from 5×10^6 to 6.3×10^5 was incubated with siRNA-CPP complexes at optimal complex-forming molar ratios; total volume was 25 μL in 96 well plate. For each CPP, three siRNA concentrations were tested (200, 100, and 50 nM). After 4 h of incubation at 37 °C, 5% CO_2 and 95% humidity, 75 μL of prewarmed fresh medium was added. After a total of 24 h, 10 μL of WST-1 reagent (Roche Diagnostics, Burgess Hill, U.K.) was added. After 3 h of incubation, the plates were shaken for 1 min and analyzed on the Omega FluoStar plate reader (BMG Labtech) according to manufacturer's instruction.

Membrane toxicity was determined using a Lactate Dehydrogenase (LDH) release assay. To that end, 5.3×10^6 SKNO-1 cells were spun down and resuspended in 8.4 mL of RPMI1640 containing 1% FCS to a density of 6×10^5 cells/mL. Seven 96-well plates were filled with CPP−siRNA complex solutions (one plate for each peptide). For each peptide, 6 wells were pipetted for each concentration (50 nM, 100 nM, 200 nM, 500 nM, and 1 μM). In addition, for each peptide, 3 background, 3 low and 3 high controls were added. Pure assay medium formed the background; negative and positive controls consisted of cells without substance and cells in 2% Triton X-100-supplemented assay medium, respectively. A total of 100 μL of cell suspension with 3.1×10^4 SKNO cells was added to the 100 μL in each well. After 4 h incubation at 37 °C, 5% CO_2, and 95% humidity, 100 μL of reaction mixture was added (1 mL of catalyst solution and 45 mL of dye solution, Roche) to each well. After 30 min incubation at room temperature in the dark, the plate was measured at 490 nm in a luminescence plate-reader. Cytotoxicity was calculated as ((sample value − low control)/(high control − low control)) × 100.

Statistics. Values are represented as mean ± SD of three independent experiments, unless stated otherwise.

Conflict of Interest: The authors declare no competing financial interest.

Supporting Information Available: Details on the effect of several salt-containing solutions, including 150 mM NaCl, RPMI1640, RPMI1640 + 10% FCS and RPMI1640 + 20% FCS, on the size of CPP−siRNA particles formed in these solutions. Selected figures of gel shift assays that were used as basis for Figure 2. Determination of peptide stability of R9 and TP10, confirming increased stability of TP10. Flow cytometry histograms of cells stained by association with CPP-Cy5.5siRNA nanoparticles. Membrane toxicity (LDH-assay) at higher concentrations of nanoparticles (200 nM, 500 nM and 1 μM). This material is available free of charge *via* the Internet at http://pubs.acs.org.

Acknowledgment. This work was funded and supported by the Honours Programme Medical Sciences, Radboud University, Nijmegen, The Netherlands (R.B.), the Medical Research Council DPFS programme (O.H.), the science foundation VR-NT, Sweden (U.L.), the Cancer foundation, Sweden (U.L.) and CePeP AB, Sweden (U.L.). The authors wish to thank Daniel Coleman for carefully reading the manuscript.

REFERENCES AND NOTES

1. Overington, J. P.; Al-Lazikani, B.; Hopkins, A. L. How Many Drug Targets Are There? *Nat. Rev. Drug Discovery* **2006**, *5*, 993–996.
2. de Fougerolles, A.; Vornlocher, H. P.; Maraganore, J.; Lieberman, J. Interfering with Disease: A Progress Report on siRNA-based Therapeutics. *Nat. Rev. Drug Discovery* **2007**, *6*, 443–453.
3. Allerson, C. R.; Sioufi, N.; Jarres, R.; Prakash, T. P.; Naik, N.; Berdeja, A.; Wanders, L.; Griffey, R. H.; Swayze, E. E.; Bhat, B.

Fully 2′-Modified Oligonucleotide Duplexes with Improved *in Vitro* Potency and Stability Compared to Unmodified Small Interfering RNA. *J. Med. Chem.* **2005**, *48*, 901–904.
4. Moschos, S. A.; Jones, S. W.; Perry, M. M.; Williams, A. E.; Erjefalt, J. S.; Turner, J. J.; Barnes, P. J.; Sproat, B. S.; Gait, M. J.; Lindsay, M. A. Lung Delivery Studies Using siRNA Conjugated to Tat(48−60) and Penetratin Reveal Peptide Induced Reduction in Gene Expression and Induction of Innate Immunity. *Bioconjugate Chem.* **2007**, *18*, 1450–1459.
5. Foged, C. siRNA Delivery with Lipid-Based Systems: Promises and Pitfalls. *Curr. Top. Med. Chem.* **2012**, *12*, 97–107.
6. Musacchio, T.; Torchilin, V. P. Recent Developments in Lipid-based Pharmaceutical Nanocarriers. *Front. Biosci.* **2011**, *16*, 1388–1412.
7. Vader, P.; van der Aa, L. J.; Storm, G.; Schiffelers, R. M.; Engbersen, J. F. Polymeric Carrier Systems for siRNA Delivery. *Curr. Top. Med. Chem.* **2012**, *12*, 108–119.
8. Gao, Y.; Liu, X. L.; Li, X. R. Research Progress on siRNA Delivery with Nonviral Carriers. *Int. J. Nanomed.* **2011**, *6*, 1017–1025.
9. Choi, Y. S.; Lee, J. Y.; Suh, J. S.; Kwon, Y. M.; Lee, S. J.; Chung, J. K.; Lee, D. S.; Yang, V. C.; Chung, C. P.; Park, Y. J. The Systemic Delivery of siRNAs by a Cell Penetrating Peptide, Low Molecular Weight Protamine. *Biomaterials* **2010**, *31*, 1429–1443.
10. Heitz, F.; Morris, M. C.; Divita, G. Twenty Years of Cell-Penetrating Peptides: From Molecular Mechanisms to Therapeutics. *Br. J. Pharmacol.* **2009**, *157*, 195–206.
11. Jafari, M.; Chen, P. Peptide Mediated siRNA Delivery. *Curr. Top. Med. Chem.* **2009**, *9*, 1088–1097.
12. Jarver, P.; Mager, I.; Langel, U. *In Vivo* Biodistribution and Efficacy of Peptide Mediated Delivery. *Trends Pharmacol. Sci.* **2010**, *31*, 528–535.
13. Crombez, L.; Divita, G. A Non-Covalent Peptide-Based Strategy for siRNA Delivery. *Methods Mol. Biol.* **2011**, *683*, 349–360.
14. Wagstaff, K. M.; Jans, D. A. Protein Transduction: Cell Penetrating Peptides and Their Therapeutic Applications. *Curr. Med. Chem.* **2006**, *13*, 1371–1387.
15. Vives, E.; Brodin, P.; Lebleu, B. A Truncated Hiv-1 Tat Protein Basic Domain Rapidly Translocates through the Plasma Membrane and Accumulates in the Cell Nucleus. *J. Biol. Chem.* **1997**, *272*, 16010–16017.
16. Wender, P. A.; Mitchell, D. J.; Pattabiraman, K.; Pelkey, E. T.; Steinman, L.; Rothbard, J. B. The Design, Synthesis, and Evaluation of Molecules that Enable or Enhance Cellular Uptake: Peptoid Molecular Transporters. *Proc. Natl. Acad. Sci. U.S.A.* **2000**, *97*, 13003–13008.
17. Futaki, S.; Suzuki, T.; Ohashi, W.; Yagami, T.; Tanaka, S.; Ueda, K.; Sugiura, Y. Arginine-rich peptides. An Abundant Source of Membrane-permeable Peptides Having Potential as Carriers for Intracellular Protein Delivery. *J. Biol. Chem.* **2001**, *276*, 5836–5840.
18. Duchardt, F.; Ruttekolk, I. R.; Verdurmen, W. P.; Lortat-Jacob, H.; Burck, J.; Hufnagel, H.; Fischer, R.; van den Heuvel, M.; Lowik, D. W.; Vuister, G. W.; *et al.* A Cell-Penetrating Peptide Derived from Human Lactoferrin with Conformation-Dependent Uptake Efficiency. *J. Biol. Chem.* **2009**, *284*, 36099–36108.
19. Lindgren, M.; Gallet, X.; Soomets, U.; Hallbrink, M.; Brakenhielm, E.; Pooga, M.; Brasseur, R.; Langel, U. Translocation Properties of Novel Cell Penetrating Transportan and Penetratin Analogues. *Bioconjugate Chem.* **2000**, *11*, 619–626.
20. Mae, M.; El Andaloussi, S.; Lundin, P.; Oskolkov, N.; Johansson, H. J.; Guterstam, P.; Langel, U. A Stearylated Cpp for Delivery of Splice Correcting Oligonucleotides Using a Non-Covalent Co-incubation Strategy. *J. Controlled Release* **2009**, *134*, 221–227.
21. El-Andaloussi, S. E.; Lehto, T.; Mager, I.; Rosenthal-Aizman, K.; Oprea, I. I.; Simonson, O. E.; Sork, H.; Ezzat, K.; Copolovici, D. M.; Kurrikoff, K.; *et al.* Design of a Peptide-Based Vector, Pepfect6, for Efficient Delivery of siRNA in Cell Culture and Systemically *in Vivo*. *Nucleic Acids Res.* **2011**, *39*, 3972–3987.
22. Ezzat, K.; Andaloussi, S. E.; Zaghloul, E. M.; Lehto, T.; Lindberg, S.; Moreno, P. M.; Viola, J. R.; Magdy, T.; Abdo, R.; Guterstam, P.; *et al.* Pepfect 14, a Novel Cell-penetrating Peptide for Oligonucleotide Delivery in Solution and as Solid Formulation. *Nucleic Acids Res.* **2011**, *39*, 5284–5298.
23. Lundin, P.; Johansson, H.; Guterstam, P.; Holm, T.; Hansen, M.; Langel, U.; El Andaloussi, S. Distinct Uptake Routes of Cell-penetrating Peptide Conjugates. *Bioconjugate Chem.* **2008**, *19*, 2535–2542.
24. Shiraishi, T.; Nielsen, P. E. Improved Cellular Uptake of Antisense Peptide Nucleic Acids by Conjugation to a Cell-penetrating Peptide and a Lipid Domain. *Methods Mol. Biol.* **2011**, *751*, 209–221.
25. Mae, M.; Andaloussi, S. E.; Lehto, T.; Langel, U. Chemically Modified Cell-Penetrating Peptides for the Delivery of Nucleic Acids. *Expert Opin. Drug Delivery* **2009**, *6*, 1195–1205.
26. El-Andaloussi, S.; Jarver, P.; Johansson, H. J.; Langel, U. Cargo-Dependent Cytotoxicity and Delivery Efficacy of Cell-Penetrating Peptides: A Comparative Study. *Biochem. J.* **2007**, *407*, 285–292.
27. Tunnemann, G.; Martin, R. M.; Haupt, S.; Patsch, C.; Edenhofer, F.; Cardoso, M. C. Cargo-Dependent Mode of Uptake and Bioavailability of Tat-Containing Proteins and Peptides in Living Cells. *FASEB J.* **2006**, *20*, 1775–1784.
28. Matozaki, S.; Nakagawa, T.; Kawaguchi, R.; Aozaki, R.; Tsutsumi, M.; Murayama, T.; Koizumi, T.; Nishimura, R.; Isobe, T.; Chihara, K. Establishment of a Myeloid Leukaemic Cell Line (SKNO-1) from a Patient with t(8;21) Who Acquired Monosomy 17 during Disease Progression. *Br. J. Hamaetol.* **1995**, *89*, 805–811.
29. Dunne, J.; Cullmann, C.; Ritter, M.; Soria, N. M.; Drescher, B.; Debernardi, S.; Skoulakis, S.; Hartmann, O.; Krause, M.; Krauter, J.; *et al.* siRNA-mediated AML1/MTG8 Depletion Affects Differentiation and Proliferation-Associated Gene Expression in t(8;21)-Positive Cell Lines and Primary AML Blasts. *Oncogene* **2006**, *25*, 6067–6078.
30. Rejman, J.; Oberle, V.; Zuhorn, I. S.; Hoekstra, D. Size-Dependent Internalization of Particles *via* the Pathways of Clathrin- and Caveolae-Mediated Endocytosis. *Biochem. J.* **2004**, *377*, 159–169.
31. Zhang, S.; Li, J.; Lykotrafitis, G.; Bao, G.; Suresh, S. Size-dependent Endocytosis of Nanoparticles. *Adv. Mater.* **2009**, *21*, 419–424.
32. Maeda, H. Tumor-Selective Delivery of Macromolecular Drugs *via* the EPR Effect: Background and Future Prospects. *Bioconjugate Chem.* **2010**, *21*, 797–802.
33. Veiman, K. L.; Mager, I.; Ezzat, K.; Margus, H.; Lehto, T.; Langel, K.; Kurrikoff, K.; Arukuusk, P.; Suhorutsenko, J.; Padari, K. Pepfect14 Peptide Vector for Efficient Gene Delivery in Cell Cultures. *Mol. Pharmaceutics* **2013**, *10*, 199–210.
34. Ezzat, K.; Helmfors, H.; Tudoran, O.; Juks, C.; Lindberg, S.; Padari, K.; El-Andaloussi, S.; Pooga, M.; Langel, U. Scavenger Receptor-Mediated Uptake of Cell-penetrating Peptide Nanocomplexes with Oligonucleotides. *FASEB J.* **2012**, *26*, 1172–1180.
35. Haupenthal, J.; Baehr, C.; Kiermayer, S.; Zeuzem, S.; Piiper, A. Inhibition of RNAse a Family Enzymes Prevents Degradation and Loss of Silencing Activity of siRNAs in Serum. *Biochem. Pharmacol.* **2006**, *71*, 702–710.
36. Hancock, R. E. Cationic Peptides: Effectors in Innate Immunity and Novel Antimicrobials. *Lancet Infect. Dis.* **2001**, *1*, 156–164.
37. Ziegler, A.; Seelig, J. Binding and Clustering of Glycosaminoglycans: A Common Property of Mono- and Multivalent Cell-Penetrating Compounds. *Biophys. J.* **2008**, *94*, 2142–2149.
38. Anko, M.; Majhenc, J.; Kogej, K.; Sillard, R.; Langel, U.; Anderluh, G.; Zorko, M. Influence of Stearyl and Trifluoromethylquinoline Modifications of the Cell Penetrating Peptide TP10 on Its Interaction with a Lipid Membrane. *Biochim. Biophys. Acta* **2012**, *1818*, 915–924.
39. El-Andaloussi, S.; Johansson, H. J.; Lundberg, P.; Langel, U. Induction of Splice Correction by Cell-Penetrating Peptide Nucleic Acids. *J. Gene Med.* **2006**, *8*, 1262–1273.